Comparison of equations-of-state with P--T experimental data of binary mixtures rich in CO2 under the conditions of pipeline transport

Comparison of Equations-of-State with P-ρ-T experimental data of binary mixtures rich in CO_2 under the conditions of pipeline transport.

Michela Mazzoccoli,[a] Barbara Bosio,[a] Elisabetta Arato,[a] Stefano Brandani[b]

[a]Department of Civil, Chemical and Environmental Engineering, University of Genoa, Via Opera Pia 15, 16145 Genoa, Italy

[b]Scottish Carbon Capture and Storage, School of Engineering, University of Edinburgh, The King's Buildings, Mayfield Road, EH9 3JL, Edinburgh, UK

Abstract

Transport of carbon dioxide is an essential feature of Carbon Capture and Storage. Power plants and industrial production plants – large point sources of CO_2 – are often situated far away from storage locations, thus it is necessary to transport the resulting CO_2-rich streams from the point of capture to the storage/utilization site. The CO_2 quality required for transport may influence the choice of the capture technology and impose limits on the performance requirements.

In order to design CO_2 transport networks, it is important to have an accurate knowledge of the thermodynamic properties of CO_2-rich mixtures containing small amounts of impurities. However, a suitable equation of state under the appropriate conditions for pipeline transport has not been clearly defined yet and different options may be used for different applications. For a quick evaluation of transport options, simple cubic EOS may be sufficient, but for accurate measurements of CO_2 flows needed for fiscal purposes more accurate non-analytical EOS may be required.

In this paper the results of different EOS, including both cubic equations and non-analytical equations, have been compared with *P-ρ-T* experimental data of binary mixtures of carbon dioxide with nitrogen, oxygen and argon obtained by the authors at the Energy and Environmental Laboratory of Piacenza (LEAP). Moreover a refitting of the mixture binary interaction parameters has been carried out for analysed EOS.

The Lee-Kesler-Plöcker, the Perturbated-Chain SAFT equations and the GERG model showed good prediction of the density of CO_2-mixtures in the conditions typical of pipeline transport: "dense" liquid phase (*P* above the critical pressure and *T* below the critical temperature) and CO_2 molar concentration greater than 95%.

Finally, the application of EOS to CO_2 transport simulations and pipeline design has been performed in order to find the best configuration of pipelines on the basis of geometrical characteristics and operating conditions.

Keywords: CO_2 mixtures; Equations of State; Volumetric Data; CO_2 Transport.

1. Introduction

For a sustainable development, energy services must be provided with low environmental impacts and low greenhouse gas (GHG) emissions.
GHG emissions, in particular CO_2 emissions, are the main cause of climate change and are related to the global use of fossil fuels for energy supply: in 2008, they provided 85% of the total amount of primary energy [1].
CO_2 emissions must decrease from 50% to 85% by 2050 compared to the levels of year 2000 and begin to decrease no later than 2015 in order to limit global average temperature increase and to avoid adverse impacts of climate change on water resources, ecosystems, food security and human health [1].
To reduce the emission levels, Intergovernmental Panel on Climate Change (IPCC) has identified a number of ways to use low-carbon energy sources while still providing energy services. Among this portfolio of technologies, the Carbon Capture and Storage (CCS) process has been proposed to prevent CO_2 emissions from post-combustion or industrial process entering the atmosphere [1,2].
Transportation is an essential component of the full CCS chain as CO_2 must be transported from power and industrial production plants to storage/utilization sites.
In order to limit corrosion rates, the gas has to be sufficiently dry, since should there be the presence of free water, CO_2 can dissolve in the water and form carbonic acid which is corrosive. In addition, the presence of free water can lead to hydrate formation which causes pipeline problems, including plugging and equipment damage [3]. Therefore water needs to be removed from the CO_2-mixture streams before transport. The CO_2 quality recommendation reported in [3] indicates that the maximum H_2O concentration should be 500 ppm. Aspelund and Jordal [4] stated that most water can be removed by means of vapour-liquid separator drums. With a proper design, this technology enables water removal down to roughly 400-500 ppm. In order to further decrease the water content, after using the separator drums, the CO_2-rich stream can be dried by regenerative adsorption columns.
In addition, for final safe storage, a CO_2 molar concentration of over 95 % is required [3], thus the CO_2-mixture must have high purity levels and the requirement for transportation may also influence the type of capture technology chosen.
Once CCS develops to a large industry, the main transport solution will be via pipelines where the CO_2-rich streams will most likely be transported in the "dense" liquid phase (above the critical pressure, P_c, and below the critical temperature, T_c) or supercritical phase, as also suggested by [4-7] . This solution makes it so that the volumes to be transported are not large and the work required in the pumping stations is reduced.
In order to design CO_2 transport networks, it is important to have an accurate knowledge of the thermodynamic properties of CO_2- rich mixtures containing small amounts of impurities (i.e. N_2, O_2, Ar, CH_4, H_2).
Therefore, studying Equations-of-State (EOS) that calculate the thermodynamic property of different mixture compositions, and finding the proper EOS for CO_2-rich mixtures could be of great interest in the CCS process. The accuracy required will also depend on the final application, and it is envisaged that more advanced EOS will be needed for fiscal metering.
This work reports the ability of different EOS, including both cubic equations and non-analytical equations, to predict the densities of CO_2-rich binary mixtures, in particular comparing EOS with P-ρ-T experimental data obtained by the authors at the Energy and Environmental Laboratory of Piacenza (LEAP). The studied binary mixtures were CO_2-N_2, CO_2-O_2 and CO_2-Ar mixtures in the liquid and vapour phases at different temperatures (273.15 K, 283.15 K and 293.15 K) and for the pressure range 1 to 20 MPa [8]. Moreover volumetric data of the same binary mixtures in supercritical conditions have been obtained at LEAP by Mantovani et al [9].
In literature, several references are already available on EOS for CO_2 and CO_2 mixtures [10-14]. However in [10, 11] only cubic equations have been compared, in [12] EOS have been studied for supercritical fluid extraction. The EOS showed in [13] have been developed for conditions different from that encountered in

pipeline transport (high CO_2 concentration). Or even, to our knowledge, no experimental data on the volume of CO_2-O_2 and few data on volume of CO_2-Ar have been used in previous works for the EOS comparison in operating conditions useful for CCS applications [14].
For the comparison between the EOS results and the *P-ρ-T* measurements and for the refitting of the mixture binary interaction parameters, the commercial simulation software Aspen Plus was used.
The results were used to assess the best configuration and the pumping station requirements of a representative pipeline.

2. Equations of State

The *P-ρ-T* experimental data of CO_2-rich mixtures, obtained at LEAP using the vibrating tube densimeter Anton Paar DMA 512-HPM [8], were compared with different EOS included in the software Aspen Plus©, one of the most used software in process engineering for the thermodynamic calculations.
The EOS analysed were chosen on the basis of a preliminary comparison, based on literature experimental data carried out by the authors [15] and results reported in a PhD thesis [16]. Both cubic and non-analytical equations, summarized in Table 1, were studied.
The cubic equations chosen were Peng Robinson (PR) [17] and Redlich Kwong Soave (RKS) [17]. These EOS contain the alpha function that gives the dependence of attractive term on temperature. In literature several models have been proposed, in this work the standard alpha function, $\alpha(T)$, has been selected (Table 1) because its modifications, in previous studies [16], did not seem to improve significantly the EOS behaviour in the density prediction.
As the CO_2 will be transported in liquid or supercritical phase, also the RKS model with volume translation, a concept introduced by Peneloux and Rauzy (RKSP) [18] to improve molar liquid volume calculation, was included in the study.
The non-analytical equations considered were the Benedict-Webb-Rubin-Starling (BWRS) [19], Lee-Kesler-Plöcker (LKP) [20] and GERG model [21]. The LKP EOS has been already used for mixtures containing CO_2 [12, 22, 23]. GERG model, originally developed for natural gas mixtures, accurately describes mixtures of up to 21 components, including CO_2, O_2, N_2 and Ar and generally describes gas phase and supercritical states with high accuracy [24].
In addition, a perturbation model was tested, in particular Perturbated-Chain SAFT (PC-SAFT) which seems to give good fits to liquid volumes [25].
In Tables 2-5 a list of critical parameters used in the EOS for each studied component is reported.

2.1. Mixing rules

The mixture parameters available in Aspen Plus have been adopted. They are obtained following different mixing rules developed in literature (Table 6).
For the cubic equations, the covolume and the volume translation parameter (if present) are calculated by simple linear mixing rules [17], while, for the attractive term, classical quadratic mixing rules are used, with binary interaction parameters k_{ij} that are defined depending on the components present in the mixture. More complicated mixing rules did not seem further improve the EOS behaviour [15] and, thus, they were not selected in this work.
In the BWRS equation the composition-dependent parameters are obtained according to the mixing rules reported in [19] where some parameters include k_{ij}. For the LKP equation the mixture properties are determined with the mixing rules suggested by [26] where k_{ij} are present. In the GERG model the mixture properties are calculated using the composition-dependent reducing functions for mixture density and temperature developed by [13].
It is necessary to take into account that the mixture properties used in the GERG model do not respect the invariance condition, discussed in [27], due to the asymmetric form.

In order to overcome the problem, the authors of this model introduced a second alternative mixture model [13] following the mixing rule suggested by Mathias et al. [28] for the reducing functions of multi-fluid approximations in order to respect the invariance condition.
A comparison, reported in [13], between the standard and the alternative mixture model evidenced that the latter describes most of the available thermal and caloric data of mixtures in the homogeneous region without significant differences between the two approaches. However, considerable differences were observed for natural gas mixtures rich in carbon dioxide, and the alternative mixture model seems to be less suited for this kind of mixtures. Therefore the GERG's authors concluded that the standard mixture model is of considerable advantage for the description of carbon dioxide rich natural gases, and that its deficiency caused by the problem of invariance seems to be of minor importance. Thus, also considering that in this work only CO_2-rich binary mixtures were selected, the standard mixture model were used.

3. Results and discussion

3.1. Results

The so-called "Data Regression System" option of Aspen Plus [29] was used both to evaluate the accuracy of selected EOS comparing the calculate results with experimental data and to fit binary interaction parameters.
This option providing the following results:

- Temperature, pressure, density and composition calculated by the equation of state models chosen by user;
- Difference between all experimental data and the calculated property;
- Relative deviation percentage between experimental data and the calculated property.

Taking into account that temperature (T), pressure (P), molar fraction (x) and density (ρ) are all measured variables and can be affected by measurement errors, these properties have been calculated using the EOS chosen and minimizing the deviation with the measured values by fitting binary interaction parameters.
For the minimization, the Maximum likelihood objective function was selected:

$$\Phi = \sum_{i=1}^{N} \left(\frac{T_{\exp,i} - T_{EOS,i}}{\sigma_{T,i}} \right)^2 + \left(\frac{P_{\exp,i} - P_{EOS,i}}{\sigma_{p,i}} \right)^2 + \left(\frac{x_{\exp,i} - x_{EOS,i}}{\sigma_{x,i}} \right)^2 + \left(\frac{\rho_{\exp,i} - \rho_{EOS,i}}{\sigma_{\rho,i}} \right)^2$$

where Φ is the objective function, N is the number of experimental data, T_{exp}, P_{exp}, x_{exp} and ρ_{exp} are the experimental temperature, pressure, molar fraction and density respectively, while T_{EOS}, P_{EOS}, x_{EOS} and ρ_{EOS} are the temperature, pressure, molar fraction and density respectively calculated by EOS and σ are the different standard deviations.
T, P and x are all measured variables and can be affected by measurement errors, thus, in the maximum likelihood objective function, errors in all variables are considered.
The objective function is minimized by manipulating the physical property parameters identified in the regression case and manipulating the estimated value corresponding to each measurement. The minimization is subject to the constraints of phase equilibrium [29].
The default standard deviations reported in Aspen Plus were used as they were similar or slightly precautionary as regards the level of uncertainty in the measurements ($\sigma_{T,i}$ = 0.1 K, $\sigma_{P,i}$ = 0.1%, $\sigma_{x,i}$ = 0.1%, $\sigma_{\rho,i}$ = 1%,).
To solve the minimization problem, the Britt-Luecke algorithm [30], a rigorous maximum-likelihood method was used.
In order to compare the different models, some dimensionless parameters were taken into account: the percentage relative deviation (*RD*) and the percentage absolute average relative deviation (*AARD*):

$$RD_i = \frac{y_{calc,i} - y_{\exp,i}}{y_{\exp,i}} \cdot 100$$

$$AARD = \frac{1}{N} \sum_{i=1}^{N} \frac{\left| y_{calc,i} - y_{\exp,i} \right|}{y_{\exp,i}} \cdot 100$$

where $y_{calc,i}$ is the variable calculated by EOS, $y_{exp,i}$ is the experimental variable and N is the number of experimental data.

The molar fractions of the binary mixtures considered for the comparison of results of different EOS are reported in Table 7.

The discussion of the comparison results was carried out considering the density difference between the calculated and the experimental values since the temperature, pressure and molar fraction deviations were negligible.

For all the selected models, initially the binary interaction parameters k_{ij} were used as reported by default in Aspen Plus (Table 8).

In the vapour region, the density prediction was quite similar for every EOS analysed and the deviation with the experimental data was not significant; AARDs were always lower than 5.0% and often lower than 2.5%. The highest differences were noticed increasing the pressure and the impurity concentration. Moreover, these differences increased further when the temperature was high (293 K). In such cases, the mixtures come close to the mixture critical temperature (T_{Cm}); in fact, the T_{Cm} decreased compared to the T_C of pure CO_2 (≈ 304 K) with increasing concentration of impurities which had a lower T_C than CO_2.

In the liquid region, a greater deviation was observed, in general and as expected, for cubic equations, whereas non- analytical equations (except BWRS) showed, in general, a better liquid density prediction.

The PR equation tends to overestimate the density value at lower T and to underestimate it at higher T, however it overestimates the density value for every temperature considered when the CO_2 concentration is lower in the CO_2-O_2 mixture. The AARDs were below 3% for all mixtures except for the O_{2b} mixtures where the AARD was above 4%, reaching about 10% at 293 K.

The RKS equation significantly underestimates the value of the liquid density, showing AARDs often above 10%.

A lower deviation was observed for the RKSP equation compared to the RKS, as expected, because the RKSP model contains the volume translation, a concept introduced by Peneloux and Rauzy [19], which improves the prediction of molar liquid volumes.

The BWRS equation generally overestimates the density value; the deviation increased when the temperature increased and the pressure decreased.

The GERG model, the LKP and PC-SAFT equations seemed to predict better the liquid density showing AARDs below 2%, except in some cases. For PC-SAFT in the case of CO_2-O_2 mixtures: AARD = 2.7 for O_{2a} and AARD = 5.1 for O_{2b}; for GERG model in the case of O_{2b} mixture at 293 K: AARD = 4%; for LKP equation in the case of the N_{2b} mixture again at 293 K: AARD = 3%. Higher AARD may be due to the fact that these mixtures are near T_{Cm}.

In order to further improve the EOS prediction, in particular for the liquid phase, the regression of binary interaction parameters was carried out.

All EOS considered were calibrated with regard to the binary interaction parameters, except the GERG model. This was due to the complexity of its binary mixture models that require a large number of experimental data in order to achieve statistical significance in the derived interaction parameters.

Table 9 reports the new k_{ij} obtained.

In the vapour region, AARDs did not significantly change: they were always lower than 5.0% and often lower than 2.5% (Table 10-15). The highest differences continued to be noticed when increasing the pressure and the impurity concentration. However, it is important to take into account that the vapour density

prediction was not the aim of this work because the CO_2-mixture will very likely be transported as a "dense" liquid phase.
A significant improvement of the liquid density prediction by EOS was noticed (Table 10-15), in particular by cubic equations that initially had reported the highest deviations.
The PR equation was still the best among the cubic equations: AARDs were always lower than 3%.
The RKS equation improved the liquid density prediction. AARDs were almost always lower than 10%, even though they remained high.
The BWRS equation, in general, showed a better density prediction, however the deviation was relatively high when the temperature increased (AARDs= 4÷5%).
The LKP equation showed low deviation also for N_{2b} mixture at 293 K (AARD ≈ 1.4%). In addition, the AARDs were always lower than 2.0%, often lower than 1.5%.
The PC-SAFT equation improved the density prediction also for CO_2-O_2 mixtures: AARD = 1.8 for O_{2a} and AARD = 3.6 for O_{2b}.
A comparison between AARDs obtained for the liquid density of the various binary mixtures for the different EOS with the k_{ij} defined by default and the fitted k_{ij} is reported in Figs. 1-3.
Figs. 4-9 show RDs in terms of the liquid density for EOS with fitted k_{ij} against the experimental value at fixed temperatures (273.15 K, 283.15 K and 293.15 K). As regards the GERG model, RDs obtained with the default mixture parameters are reported since this model has not been calibrated as regards the binary interaction parameters.

3.2. Discussion

An improved liquid density prediction was achieved with the RKS equation after the regression of the binary interaction parameters, k_{ij} . It is clear that density predictions are not recommended for CO_2 mixtures with k_{ij} = 0 [31]. However, its AARDs continued to be the highest among all the equations considered in this study. This was also observed for CO_2-mixtures by Duan et al. [23] who studied the CH_4-CO_2 mixture and found that this equation gave poor prediction of molar volumes in the CO_2-rich phase.
In general, the cubic equations showed higher errors. Cubic EOS were developed originally to describe the non-ideal behaviour in the vapour region and were extended to describe the liquid region as well. However, without volume translation the prediction of liquid density can lead to significant deviations, as also reported in [12]. Only the PR equation seemed to be accurate in density prediction, confirming the results reported in [9, 12].
Among the non-analytical EOS, the LKP and the PC-SAFT equations showed lower AARDs than the BWRS equation. Also Yang et al [12] stated that Lee Kesler is an accurate equation for CO_2 mixtures.
The LKP equation predicted the liquid density of CO_2-Ar and CO_2-O_2 mixtures accurately with the k_{ij} fixed by default. For these mixtures the calibration of the binary interaction parameters did not lead to an improvement of the density prediction. The fitted k_{ij} allowed a significant reduction of AARDs for the CO_2-N_2 mixtures.
A similar consideration can be made for the PC-SAFT equation. The liquid density of CO_2-Ar and CO_2-N_2 mixtures was accurately predicted also with the default k_{ij}, whereas the fitted binary interaction parameters enabled a reduction of AARDs for the CO_2-O_2 mixtures. However, in this case AARDs remained higher than that of the LKP equation.
It should be noted that in this study the aim is to improve the prediction of the liquid density in order to study the conditions typical for transport in pipelines, so the phase equilibrium envelope was not used in the parameter regression. If accurate predictions of both density and phase equilibria are required, then the volume translation should be used.
In conclusion, among the equations tested with the fitted k_{ij} parameters, the LKP and PC-SAFT equations showed accurate density predictions, and the GERG model seemed to well predict the liquid density, even if its binary interaction parameters were not fitted to the same set of data; in particular, this was evidenced in

the conditions typical for transport in pipelines where the CO_2-mixture should be characterised by a CO_2 molar concentration above 95%.

4. Application of EOS to CO_2 transport simulations

The results of the EOS comparison are useful when applying the thermodynamic models for the simulation of CO_2 transport in a pipeline. An EOS is necessary to determine, on the basis of operating conditions and composition, when a phase change occurs along the pipeline transporting a CO_2-rich mixture. This in turn enables to determine where a pumping station is needed in order to avoid an excessive pressure decrease (lower than the mixture critical pressure, P_{Cm}) and the formation of a two-phase fluid or an important density variation.

At first, the transport of pure CO_2 was simulated using the software program Aspen Plus® and the Span and Wagner equation [32], the most accurate model currently available for pure CO_2.

Fig. 10 reports the altimetric profile of the simulated pipeline; it was similar to that of a real onshore oil pipeline, as provided by the company ABB. The pipeline was buried and 520 km long, its maximum altitude gap was 860 m.

A wide range of T_a were studied in order to consider the possible temperature variations throughout the year in different regions: 253 K, 273 K, 283 K, 303 K and 323 K.

In addition, different T_i (273 K, 283 K, 293 K and 303 K) and various pipeline diameters D and thicknesses were considered (Table 16) in order to find the best configuration. The pipeline thickness was calculated by means of the criteria for pressure design of piping components reported in [33]. The overall heat coefficient was determined by the equation for a composite cylindrical pipe wall reported in [34] considering that the pipeline was surrounded by 1 m of soil.

When T_a is high (323K), the CO_2 is in a supercritical region. In order to avoid a significant density decrease of the fluid, it is necessary to stay above the CO_2 critical pressure, 7.4 MPa [35]. When the temperature is lower, a pressure lower than P_C could be acceptable, provided that it remains in the liquid phase. However, as the pipeline could be subject to different ambient temperatures throughout the year, it would always be better to transport the CO_2 at P higher than 7.4 MPa. Therefore, four pumping stations were inserted and their locations have been chosen on the basis of the pressure drop, avoiding to reach 8 MPa.

The pressure drop along the pipeline with D = 0.618 m at different T_a and T_i is reported in Fig. 11. This shows how the pump introduction enabled to increase the fluid pressure and to maintain the pressure values higher than 7.4 MPa.

Figs. 12-14 show the density profile along the pipeline with D = 0.618 m at different T_a and T_i, while Fig. 15 reports the density profile at T_a = 283 K and at different T_i and D.

On the basis of the obtained results, a lower T_i avoids lower values of density, in particular when T_a is high (323K), but a lower temperature requires a significant fluid cooling.

A bigger pipeline diameter seems to be better, but if the diameter is bigger, the pipeline thickness is bigger as well and the cost could be higher.

Therefore a pipeline configuration which could be a good compromise between different problems is a pipeline with D= 0,618 m and Ti = 283 K. Table 17 reports the characteristics of the configuration selected among those considered.

Simulations of CO_2-mixtures in the same pipeline were then carried out using the EOS that seemed to better predict the experimental density: GERG model, LKP and PC-SAFT equations.

Table 18 shows the molar fractions of the CO_2-mixtures considered in the transport simulations.

The equations showed similar results as regards CO_2-Ar mixtures, as evident in Fig. 16 where the density profiles along the pipeline for CO_2-Ar mixture with x_{Ar}= 0.04 are displayed.

In the other cases (Figs. 17-18), the density profiles were similar. However, as regards CO_2-O_2 mixtures, the density values reported by the PC-SAFT equation were lower compared to the values of other EOS (about

2.2%), while, as regards CO_2-N_2 mixtures, the density values reported by the LKP equation were higher compared to the values of other EOS (about 2.5%). These results confirm what reported in 3.2.
In addition the simulation results showed the importance of taking into account the impurity concentration in the pipeline design. In fact, for each binary mixture studied, if the impurity concentration increased, the density and the pressure decreased more along the pipeline. An example for CO_2-N_2 mixtures is showed in Fig 19.
For all the considered impurities, P_{Cm} increased when the CO_2 concentration decreased. Thus in the case of binary mixtures, the simulation results evidenced that an extra pumping station is necessary for the pipeline geometry considered (Fig. 20). In this way, the mixture (also when the impurity concentration is higher) is above the mixture critical point. Fig. 21 reports an example for CO_2-Ar mixtures at different argon molar fraction and at ambient temperature = 323 K. T_{Cm} and P_{Cm} values of the mixtures displayed in Fig. 21 are reported in Table 19 and were calculated by empirical methods presented in [35].
It is important to consider that the minimum P to guarantee the existence of the only liquid phase can be different from P_{Cm} by several percentage points. Therefore, as it can be difficult to evaluate the mixture PT envelope near the critical region with accuracy and reliability, it may be useful as a precautionary measure for the pipeline geometry considered to insert an additional pumping station or to increase the inlet pressure.

5. Conclusions

This study presented a comparison between new P-ρ-T measurements of CO_2-binary mixtures with argon, nitrogen and oxygen obtained at LEAP and density values calculated by different EOS (PR, RKS, RKSP, BWRS, LKP, PC-SAFT and GERG).
In addition, new binary interaction parameters were regressed for all EOS considered except the GERG model.
The GERG model, the LKP and PC-SAFT equations evidenced a good prediction of liquid density in particular in the conditions typical of CO_2-mixture pipeline transport (CO_2 concentration $\geq$ 95%).
Regarding the cubic equations, the PR seemed the most accurate.
Simulations of a representative pipeline for transport of different CO_2-rich binary mixtures were presented. The pipeline geometry was set to a configuration similar to a real oil pipeline. The pressure drop along the pipeline was studied in order to evaluate where pumping stations should be inserted so as to avoid the formation of a two-fluid phase or an important density decrease, which can cause problems to transport in pipelines.
The simulation results evidenced that small increases of impurity concentration in the mixture (molar fraction of impurities from 0.02 to 0.05) can cause variations of thermodynamics properties, leading to additional pumping station requirements.
The approach presented suggests how evaluate different pipeline configurations to optimize the operating conditions (i.e. inlet fluid temperature and pressure, “dense” liquid phase or supercritical phase) on the basis of altimetry profile, length of pipeline and impurity concentrations.
In addition this study can be useful to determine the proper requirements of a CO_2 purification/conditioning unit before the final pipeline transport.

Acknoledgments
The authors wish to thank Prof. G. Soave for his precious suggestions regarding the study of EOS, and the company ABB for its availability in providing data for the pipeline simulations.

References
[1] O.Edenhofer, R. Pichs-Madruga, Y. Sokona, K. Seyboth, P. Matschoss, S. Kadner, T. Zwichel, P. Eiclemeier, G. Hansen, S. Schlömer, C. von Stechow, IPCC Special Report on Renewable Energy Sources

and Climate Change Mitigation, Cambridge University Press, Cambridge, United Kingdom and New York, NY, USA, 2011.
[2] Climate Change 2007: Synthesis Report. Contribution of Working Groups I, II and III to the Fourth Assessment Report of the Intergovernmental Panel on Climate Change [Core Writing Team, Pachauri, R.K and Reisinger, A. (eds.)]. IPCC, Geneva, Switzerland, 2007.
[3] E. De Visser, C. Hendriks, M. Barrio, M.J.Mølnvik, G. De Koeijer, S. Liljemark, Y. Le Gallo, Dynamis CO_2 quality recommendations, International Journal of Greenhouse Gas Control 2 (2008) 478-484.
[4] A. Aspelund, K. Jordal, Gas conditioning – The interface between CO_2 capture and transport, International Journal of Greenhouse Gas Control 1 (2007) 343-354.
[5] IPCC Special Report, Carbon Dioxide Capture and Storage. IPCC, 2005.
[6] J. Gale, J. Davison. Transmission of CO_2 – safety and economic considerations, Energy, 29 (2004) 1319–1328.
[7] A. Cosham and R. J. Eiber, Fracture propagation in CO_2 pipeline, Journal of Pipeline Engineering (2007), 147-158.
[8] M. Mazzoccoli, B. Bosio, E. Arato, Pressure-density-temperature measurements of binary mixtures rich in CO_2 for pipeline transportation in the CCS process, Journal of Chemical and Engineering Data 57(2012), 2774-2783.
[9] M. Mantovani, P. Chiesa, G. Valenti, M. Gatti, S. Consonni, Supercritical pressure-density-temperature measurements on CO_2-N_2, CO_2-O_2 and CO_2-Ar binary mixtures, Journal of Supercrit. Fluids. 61 (2012) 34-43.
[10] H. Li, J. Yan, Evaluating cubic equations of state for calculation of vapour-liquid equilibrium of CO_2 and CO_2-mixtures for CO_2 capture and storage processes. Applied Energy, 86 (2009) 826-836.
[11] H. Li, J. Yan, Impacts of equations of state (EOS) and impurities on the volume calculation of CO_2 mixtures in the applications of CO_2 capture and storage (CCS) processes, Applied Energy, 86 (2009) 2760-2770.
[12] J. Yang, P. R. Griffiths, A. R.H. Goodwin, Comparison of methods for calculating thermodynamic properties of binary mixtures in the sub and super critical state: Lee–Kesler and cubic equations of state for binary mixtures containing either CO_2 or H_2S, Journal of Chemical Thermodynamics, 35 (2003) 1521–1539.
[13] O. Kunz, R. Klimeck, W. Wagner, M. Jaeschke, The GERG-2004 Wide-Range Equation of State for Natural Gses and Other Mixtures, GERG Technical Monograph 15 (2007).
[14] Ø. Wilhelmsen, G. Skaugen, O. Jørstad, H. Li, Evaluation of SPUNG# and other Equations of State for use in Carbon Capture and Storage modelling, Energy Procedia, 23 (2012) 236 – 245.
[15] M. Mazzoccoli, B. Bosio, E. Arato, Analysis and comparison of Equations-of-State with p-ρ-T experimental data for CO_2 and CO_2-mixture pipeline transport, Energy Procedia 23 (2012), 274-283.
[16] M. Mazzoccoli, Carbon Capture, Storage and Transportation (CCS&T) process: general aspects and focus on CO_2 pipeline modelling, PhD thesis, University of Genoa, 2011.
[17] B.E. Poiling, J.M. Prausnitz, J.P. O'Connell, The Properties of Gases and Liquids, 5th ed., McGraw-Hill, 2007.
[18] A. Peneloux, E. Rauzy, R. Freze, A consistent correlation for Redlich-Kwong-Soave volumes, Fluid Phase Equilibria 8 (1982) 7-23.
[19] K.E. Starling, M. S. Han, Thermo data refined for LPG, part 14: mixtures, Hydrocarbon Processing (1972) 129-132.
[20] H. Knapp, R. Döring, L. Oellrich, U. Plöcker, J.M. Prausnitz, Vapor-liquid equilibria for mixtures of low boiling substances, Vol. VI, Dechema Deutsche Gesellschaft für Chemisches Apparatewesen, 1982.
[21] O. Kunz, W. Wagner, The GERG-2008 wide-range equation of state for natural gases and other mixtures: an expansion of GERG-2004, Journal of Chemical and Engineering, 57 (2012), 3082-3091.
[22] Z. Duan, N. Møller, J. H. Weare, An equation of state for the CH_4-CO_2-H_2O system: II. Mixtures from 50 to 1000°C and 0 to 1000 bars, Geochimica et Cosmochimica Acta, 56 (1992) 2619-2631.

[23] Z. Duan, N. Møller, J. H. Weare, An equation of state for the CH_4-CO_2-H_2O system: I. Pure systems from 0 to 1000°C and 0 to 8000 bar, Geochimica et Cosmochimica Acta, 56 (1992) 2605-2617.
[24] R. Span, J. Gernert, A. Jäger, Accurate thermodynamic-property models for CO2-rich mixtures, Energy Procedia, 37 (2013) 2914 – 2922.
[25] J. Gross, G. Sadowski, Perturbed-chain SAFT: an equation of state based on a perturbation theory for chain molecules, Industrial and Engineering Chemistry Research, 40 (2001), 1244-1260.
[26] U. Plöcker, H. Knapp, J.M. Prausnitz, Calculation of high-pressure vapor-liquid equilibria from a corresponding-states correlation with emphasis on asymmetric mixtures, Industrial and Engineering Chemistry Process Design and Development, 17 (1978) 324-332.
[27] M. Michelsen, H. Kistenmacher, On composition-dependent interaction coefficients, Fluid Phase Equilibria 58 (1989) 229-230.
[28] P. Mathias, H. C. Klotz, J. M. Prausnitz, Equation-of –State mixing rules for multicomponent mixtures: the problem of invariance, Fluid Phase Equilibria 67 (1991) 31-44.
[29] Aspen Physical Property System, Aspen Tech, 2010.
[30] R. Luecke, H. Britt, The estimation of parameters in nonlinear implicit models, Technometrics, 15 (1973) 233-247.
[31] G. Soave, Equilibrium constants from a modified Redlich-Kwong equation of state, Chemical Engineering Science, 27 (1982) 1197-1203.
[32] R. Span, W. Wagner, A New Equation of State for Carbon Dioxide covering the fluid region from triple-point to 1100 K at pressures up to 800 MPa, Journal of Physical Chemistry 25 (1996) 1509-1596.
[33] ASME code for pressure piping, Pipeline transportation system for liquid hydrocarbons and other liquids, The American Society of Mechanical Engineers, 2002.
[34] R. B. Bird, W. E. Stewart, E. N. Lightfoot, Transport Phenomena, Wiley, 2007.
[35] R. H. Perry, D. W. Green, Perry's Chemical Engineers' Handbook, 8th ed., 2007.
[36] B.E. Poiling, J.M. Prausnitz, J.P. O'Connell, The Properties of Gases and Liquids, 4th ed., McGraw-Hill, 1988.

Equation	Function form	Par
PR [17]	$P = \frac{RT}{v-b} - \frac{a}{v(v+b)+b(v-b)}$	$a = \alpha\, 0.45724 \frac{R^2 T_c}{P_c}$ $\alpha(T) = [1$ $m = 0.37464 + 1$
RKS [17]	$P = \frac{RT}{v-b} - \frac{a}{v(v+b)}$	$a = \alpha\, 0.42747 \frac{R^2 T_c}{P_c}$ $\alpha(T) = [1$ $m = 0.48508 + 1$
RKSP [18]	$P = \frac{RT}{v+c-b} - \frac{a}{(v+c)(v+c+b)}$	$a = \alpha\, 0.42747 \frac{R^2 T_c}{P_c}$ $\alpha(T) = [1$ $m = 0.48508 + 1$ $c = 0.40768 \frac{R}{P}$
BWRS [19]	$P = \rho RT + \left(B_0 RT - A_0 - \frac{C_0}{T^2} + \frac{D_0}{T^3} - \frac{E_0}{T^4}\right)\rho^2 + \left(bRT - a - \frac{d}{T}\right)\rho^3 + \alpha\left(a + \frac{d}{T}\right)\rho^6 + \frac{c\rho^3}{T^2}(1+\gamma\rho^2)\exp(-\gamma\rho^2)$	$\rho_c B_0 = A_1 + B_1\omega$ $\quad \frac{\rho_c A_0}{RT_c}$ $\rho_c^2\gamma = A_4 + B_4\omega$ $\quad \rho_c^2 b$ $\rho_c^3\alpha = A_7 + B_7\omega$ $\quad \frac{\rho_c^2 c}{RT_c^3} =$ $\frac{\rho_c^2 d}{RT_c^2} = A_{10} + B_{10}\omega$ The values for the parameters A_j a
LKP [20]	$Z = Z^0 + \frac{\omega}{\omega_R}(Z^0 - Z^R)$ Z^0 and Z^R are functions of the BWR form, Z^0 is for a simple fluid and Z^R is for reference fluid n-octane [21] Z^0 or $Z^R = 1 + \frac{B}{v_r} + \frac{C}{v_r^2} + \frac{D}{v_r^5} + \frac{c_4}{T_r^3 v_r^2} + \left(\beta + \frac{\gamma}{v_r^2}\right)\exp\left(-\frac{\gamma}{v_r^2}\right)$	$v_r = \frac{P_c v}{RT_c}$ $C = c_1 - \frac{c_2}{T_r} - \frac{c_3}{T_r^2}$ The values of b_1, b_2, b_3, b_4, c_1, c_2, c_3, are rep
PC-SAFT [25]	$Z = Z^{id} + Z^{hc} + Z^{disp}$	Z^{id} is the ideal gas contribution, Z^{disp} is the perturb

Table 1. Summary of studied EOS

Equation	Function form	Par
GERG	$\alpha(\delta,\tau,x) = \alpha^0(\rho,T,x) + \alpha^r(\delta,\tau,x)$	$\delta = \frac{\rho}{\rho}$
[13-21]	$\alpha^0(\rho,T,x) = \sum_{i=1}^{N} x_i\left[\alpha_{oi}^0(\rho,T)\right] + lnx_i$	$\frac{R^*}{R}\left[\left(\frac{\rho}{\rho_{c,i}}\right) + n_{oi,1}^0 + n$
	$\alpha^r(\delta,\tau,x) = \sum_{i=1}^{N} x_i\alpha_{0i}^r(\delta,\tau) + \sum_{i=1}^{N-1}\sum_{j=i+1}^{N} x_i x_j\, F_{ij}\, \alpha_{ij}^r(\delta,\tau)$	$\sum_{k=4,6} n_{oi,k}^0 ln\left\lvert\sinh\left(\vartheta_{oi,k}^0 \frac{T_{c,i}}{T}\right)\right.$
		$\alpha_{0i}^r = \sum_{k=1}^{K_{Pol,i}} n_{oi,k}\,\delta^{d_{oi,k}}\tau^{t_{oi,k}} +$
		$\alpha_{ij}^r = \sum_{k=1}^{K_{Pol,ij}} n_{ij,k}\,\delta^{d_{ij,k}}\tau^{t_{ij,k}} + \sum_{k=K_{Pol,i}}^{K_{Pol,i}+K_{Ex}}$
		The values of all para

Table 1. (continued)

Symbols

P	Pressure
P_c	Critical pressure
R	Universal gas constant
T	Temperature
T_c	Critical temperature
T_r	Reduced temperature
v_r	Reduced molar volume
v	Molar volume
Z	Compression factor [-]
ρ	Density
ρ_c	Critical density
ρ_r	Reduced density
ω	acentric factor [-]

Other symbols are specific parameters of different EOS

Table 2. Parameters used in EOS for CO_2.

Equation	Critical temperature Tc (K)	Critical pressure Pc (MPa)	Critical compression factor Zc	Acentric factor ω
PR	304.15	7.376	0.274	0.231
RKS	304.15	7.376	0.274	0.231
RKSP	304.21	7.383	0.274	0.223621
BWRS	304.21	7.383	0.274	0.223621
LKP	304.21	7.383	0.271	0.223621
PC-SAFT	304.21	7.383	0.274	0.223621
GERG	304.21	7.383	0.274	0.223621

Table 3. Parameters used in EOS for Ar.

Equation	Critical temperature Tc (K)	Critical pressure Pc (MPa)	Critical compression factor Zc	Acentric factor ω
PR	150.71	4.864	0.291	0
RKS	150.71	4.864	0.291	0
RKSP	150.86	4.898	0.291	0
BWRS	150.86	4.898	0.291	0
LKP	150.86	4.898	0.291	0
PC-SAFT	150.86	4.898	0.291	0
GERG	150.86	4.898	0.291	0

Table 4. Parameters used in EOS for N_2.

Equation	Critical temperature Tc (K)	Critical pressure Pc (MPa)	Critical compression factor Zc	Acentric factor ω
PR	126.15	3.394	0.289	0.045
RKS	126.15	3.394	0.289	0.045
RKSP	126.2	3.4	0.289	0.0377215
BWRS	126.2	3.4	0.289	0.0377215
LKP	126.2	3.4	0.287	0.0377215
PC-SAFT	126.2	3.4	0.289	0.0377215
GERG	126.2	3.4	0.289	0.0377215

Table 5. Parameters used in EOS for O_2.

Equation	Critical temperature Tc (K)	Critical pressure Pc (MPa)	Critical compression factor Zc	Acentric factor ω
PR	154.77	7.376	0.288	0.019
RKS	154.77	7.376	0.288	0.019
RKSP	154.58	5.043	0.288	0.0221798
BWRS	154.58	5.043	0.288	0.0221798
LKP	154.58	5.043	0.288	0.0221798
PC-SAFT	154.58	5.043	0.288	0.0221798
GERG	154.58	5.043	0.288	0.0221798

Table 6. Summary of used mixing rules.

Equation	Mixing rules
PR	$a = \sum_i \sum_j x_i\, x_j (a_i a_j)^{0.5}(1-k_{ij}) \qquad b = \sum_i x_i\, b_i \qquad k_{ij} = k_{ji}$
RKS	$a = \sum_i \sum_j x_i\, x_j (a_i a_j)^{0.5}(1-k_{ij}) \qquad b = \sum_i x_i\, b_i \qquad k_{ij} = k_{ji}$
RKSP	$a = \sum_i \sum_j x_i\, x_j (a_i a_j)^{0.5}(1-k_{ij}) \qquad b = \sum_i x_i\, b_i \qquad c = \sum_i x_i\, c_i \qquad k_{ij} = k_{ji}$
BWRS	$B_0 = \sum_i x_i B_{0i} \qquad A_0 = \sum_i \sum_j x_i x_j A_{0i}^{1/2} A_{0j}^{1/2}(1-k_{ij}) \qquad C_0 = \sum_i \sum_j x_i x_j C_{0i}^{1/2} C_{0j}^{1/2}(1-k_{ij})^3$ $\gamma = \left[\sum_i x_i \gamma_i^{1/2}\right]^2 \quad b = \left[\sum_i x_i b_i^{1/3}\right]^3 \quad a = \left[\sum_i x_i a_i^{1/3}\right]^3 \quad \alpha = \left[\sum_i x_i \alpha_i^{1/3}\right]^3$ $c = \left[\sum_i x_i c_i^{1/3}\right]^3 \qquad D_0 = \sum_i \sum_j x_i x_j D_{0i}^{1/2} D_{0j}^{1/2}(1-k_{ij})^4$ $d = \left[\sum_i x_i d_i^{1/3}\right]^3 \qquad E_0 = \sum_i \sum_j x_i x_j E_{0i}^{1/2} E_{0j}^{1/2}(1-k_{ij})^5$
LKP	$V_{cm} = \sum_i \sum_j x_i\, x_j V_{cij} \qquad \omega = \sum_i x_i\, \omega_i \qquad Z = \sum_i x_i\, Z_{ci}$
GERG	$\frac{1}{\rho_r(x)} = \sum_{i=1}^{N} x_i^2 \frac{1}{\rho_{c,i}} + \sum_{i=1}^{N-1}\sum_{j=i+1}^{N} 2x_i x_j \beta_{v,ij}\gamma_{v,ij} \frac{x_i + x_j}{\beta_{v,ij}^2 x_i + x_j} \frac{1}{8}\left(\frac{1}{\rho_{c,i}^{1/3}} + \frac{1}{\rho_{c,j}^{1/3}}\right)^3$ $T_r(x) = \sum_{i=1}^{N} x_i^2 T_{c,i} + \sum_{i=1}^{N-1}\sum_{j=i+1}^{N} 2x_i x_j \beta_{T,ij}\gamma_{T,ij} \frac{x_i + x_j}{\beta_{T,ij}^2 x_i + x_j} \frac{1}{8}\left(T_{c,i} \cdot T_{c.j}\right)^{0.5}$

For PC-SAFT mixing rules see directly [25].

Table 7. Molar fraction of the considered binary mixtures.

	Ar_a	Ar_b	N_{2a}	N_{2b}	O_{2a}	O_{2b}
CO_2	0.9605	0.9276	0.9873	0.8785	0.9558	0.8512
Ar	0.0395	0.0724	-	-	-	-
N_2	-	-	0.0127	0.1215	-	-
O_2	-	-	-	-	0.0442	0.1488

Table 8. Mixture parameters k_{ij} reported by default in Aspen Plus.

	PR	RKS	RKSP	BWRS	LKP
CO_2-Ar	0	0	0	0	0
CO_2-O_2	0	0	0	0	0
CO_2-N_2	-0.017	-0.032	0	0	0.107

Table 9. Fitted k_{ij}.

	PR	RKS	RKSP	BWRS	LKP
CO_2-Ar	0.086	-0.627	-0.339	0.076	0.008
CO_2-O_2	0.192	-0.186	0.009	0.077	-0.045
CO_2-N_2	-0.069	-0.347	-0.297	-0.082	0.081

Table 10. AARDs between the density calculated by selected EOS and experimental data of Ar_a binary mixture. The results were obtained with fitted k_{ij} (except for GERG model).

	Vapour				Liquid			
	273 K	283 K	293 K	**Average**	273 K	283 K	293 K	**Average**
PR	2.0	1.3	2.1	**1.8**	2.3	1.6	2.7	**2.2**
RKS	2.3	1.2	1.9	**1.8**	6.6	7.5	8.2	**7.4**
RKSP	2.7	1.1	1.3	**1.7**	1.8	3.3	4.9	**3.3**
BWRS	2.2	1.1	1.6	**1.6**	1.4	1.9	2.9	**2.1**
LKP	2.5	1.1	1.2	**1.6**	0.7	0.6	0.6	**0.6**
PC-SAFT	3.4	1.8	1.6	**2.3**	0.5	0.3	1.0	**0.6**
GERG	2.8	1.3	1.2	**1.8**	0.8	0.4	0.2	**0.5**

Table 11. AARDs between the density calculated by selected EOS and experimental data of Ar_b binary mixture. The results were obtained with fitted k_{ij} (except for GERG model).

	Vapour				Liquid			
	273 K	283 K	293 K	**Average**	273 K	283 K	293 K	**Average**
PR	1.7	1.2	1.7	**1.5**	2.1	1.6	2.2	**2.0**
RKS	1.9	1.7	1.0	**1.5**	4.8	4.6	4.3	**4.6**
RKSP	1.2	0.8	1.0	**1.0**	1.0	1.5	2.1	**1.5**
BWRS	1.2	0.7	1.0	**1.0**	1.4	2.4	1.9	**1.9**
LKP	0.7	0.8	1.2	**0.9**	0.4	0.8	0.3	**0.5**
PC-SAFT	0.7	1.2	1.4	**1.1**	0.2	0.3	1.2	**0.6**
GERG	0.7	0.9	1.2	**0.9**	0.4	0.6	0.6	**0.5**

Table 12. AARDs between the density calculated by selected EOS and experimental data of N_{2a} binary mixture. The results were obtained with fitted k_{ij} (except for GERG model).

	Vapour				Liquid			
	273 K	283 K	293 K	**Average**	273 K	283 K	293 K	**Average**
PR	0.9	1.5	3.5	**2.0**	1.8	1.8	2.4	**2.0**
RKS	2.4	0.5	1.6	**1.5**	9.7	10.7	11.6	**10.7**
RKSP	2.5	0.5	1.6	**1.5**	4.0	5.5	6.7	**5.4**
BWRS	1.0	1.1	3.0	**1.7**	1.0	2.0	3.4	**2.1**
LKP	1.2	0.7	2.4	**1.4**	0.3	0.6	1.1	**0.7**
PC-SAFT	2.9	0.8	1.9	**1.9**	0.3	0.4	0.7	**0.5**
GERG	1.6	0.4	2.0	**1.3**	0.1	0.1	0.2	**0.1**

Table 13. AARDs between the density calculated by selected EOS and experimental data of N_{2b} binary mixture. The results were obtained with fitted k_{ij} (except for GERG model).

	Vapour				Liquid			
	273 K	283 K	293 K	**Average**	273 K	283 K	293 K	**Average**
PR	2.7	1.6	2.2	**2.2**	1.5	1.4	0.8	**1.2**
RKS	2.7	1.1	2.0	**1.9**	6.9	7.0	4.6	**6.2**
RKSP	2.7	0.8	1.6	**1.7**	2.4	2.9	3.1	**2.8**
BWRS	2.8	1.4	2.0	**2.1**	2.6	3.8	4.4	**3.6**
LKP	3.2	0.8	0.7	**1.6**	0.3	0.4	1.4	**0.7**
PC-SAFT	3.5	1.0	1.1	**1.9**	0.6	1.0	0.5	**0.7**
GERG	2.7	0.6	0.8	**1.4**	1.6	2.1	1.3	**1.7**

Table 14. AARDs between the density calculated by selected EOS and experimental data of O_{2a} binary mixture. The results were obtained with fitted k_{ij} (except for GERG model).

	Vapour				Liquid			
	273 K	283 K	293 K	**Average**	273 K	283 K	293 K	**Average**
PR	0.8	1.2	2.7	**1.6**	1.7	2.0	2.6	**2.1**
RKS	0.5	2.2	3.3	**2.0**	9.0	9.4	9.8	**9.4**
RKSP	0.8	2.6	3.8	**2.4**	4.3	5.2	6.3	**5.3**
BWRS	0.7	1.4	2.8	**1.6**	1.3	2.1	2.8	**2.1**
LKP	0.4	2.3	3.7	**2.1**	0.3	0.2	0.2	**0.2**
PC-SAFT	0.8	2.3	3.5	**2.2**	1.2	1.9	2.3	**1.8**
GERG	0.6	2.6	4.0	**2.4**	0.2	0.1	0.1	**0.1**

Table 15. AARDs between the density calculated by selected EOS and experimental data of O_{2b} binary mixture. The results were obtained with fitted k_{ij} (except for GERG model).

	Vapour				Liquid			
	273 K	283 K	293 K	**Average**	273 K	283 K	293 K	**Average**
PR	1.2	2.2	2.8	**2.1**	1.6	1.6	1.7	**1.6**
RKS	1.4	3.1	2.7	**2.4**	3.5	1.8	6.8	**4.0**
RKSP	0.6	1.5	2.5	**1.5**	1.6	1.4	4.1	**2.4**
BWRS	0.9	1.8	2.1	**1.6**	2.7	2.7	5.4	**3.6**
LKP	0.9	0.6	0.7	**0.7**	0.2	0.9	1.9	**1.0**
PC-SAFT	1.2	2.5	3.6	**2.4**	4.1	2.9	3.7	**3.6**
GERG	0.8	0.5	0.7	**0.7**	0.7	1.2	4.0	**2.0**

Table 16. Different pipe configurations considered.

Inside diameter (m)	**Thickness (m)**	**Roughness (m)**	**Overall heat transfer coefficient ($W\ m^{-2}\ K^{-1}$)**	**Flow rate ($kg\ s^{-1}$)**
0.303	0.010	0.0000475	6.1	70
0.381	0.013	0.0000475	5.2	125
0.618	0.021	0.0000475	3.8	450
0.762	0.025	0.0000475	3.3	770

Table 17. Operating conditions and pipeline characteristics of the selected configuration.

Material	Steel, API 5L X65
Max pressure (MPa)	18
Inside diameter (m)	0.618
Thickness (m)	0.021
Roughness (m)	0.0000475
Soil thickness (m)	1
Inlet fluid temperature (K)	283
Overall heat transfer coefficient ($W\ m^{-2}\ K^{-1}$)	3.8
Flow rate ($kg\ s^{-1}$)	450

Table 18. Molar fraction of the binary mixtures studied in the transport simulations.

CO_2	0.98	0.96	0.98	0.96	0.98	0.95
Ar	0.02	0.04	-	-	-	-
N_2	-	-	0.02	0.04	-	-
O_2	-	-	-	-	0.02	0.05

Table 19. Critical temperature and pressure of different CO_2-binary mixtures.

Components	CO_2 concentration	T_{Cm} (K)	P_{Cm} (MPa)
CO_2-Ar	0.98	303.29	7.71
CO_2-Ar	0.96	302.33	8.01
CO_2-N_2	0.98	303.3	7.43
CO_2-N_2	0.96	301.3	7.47
CO_2-O_2	0.98	303.37	7.69
CO_2-O_2	0.95	302.25	8.05

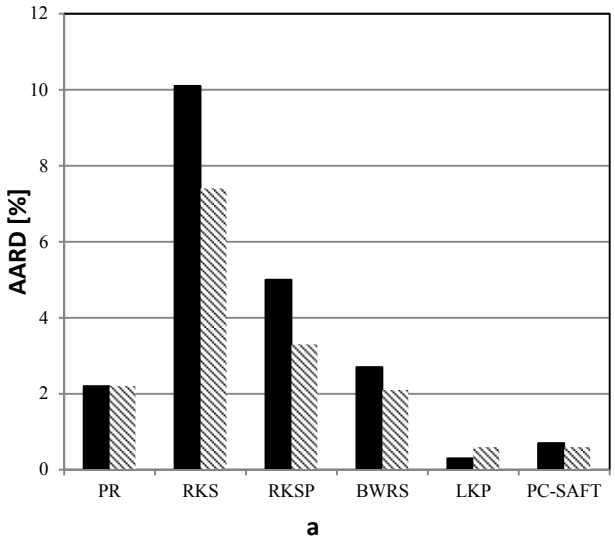

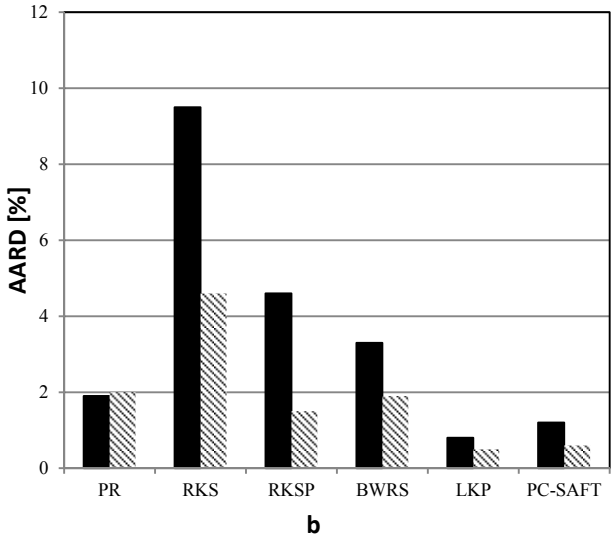

Fig. 1. AARDs between the liquid experimental density and the density calculated by EOS with k_{ij} defined in Aspen by default (■) and fitted k_{ij} (▨) for Ar_a mixture (a) and for Ar_b mixture (b).

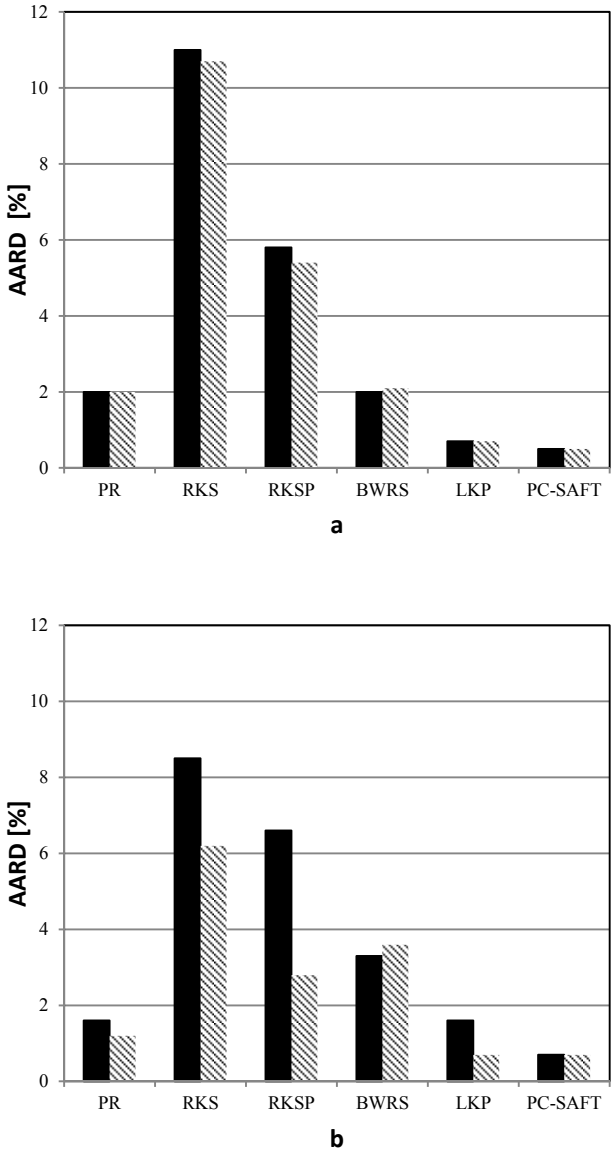

Fig. 2. AARDs between the liquid experimental density and the density calculated by EOS with k_{ij} defined in Aspen by default (■) and fitted k_{ij} (▨) for N_{2a} mixture (a) and for N_{2b} mixture (b).

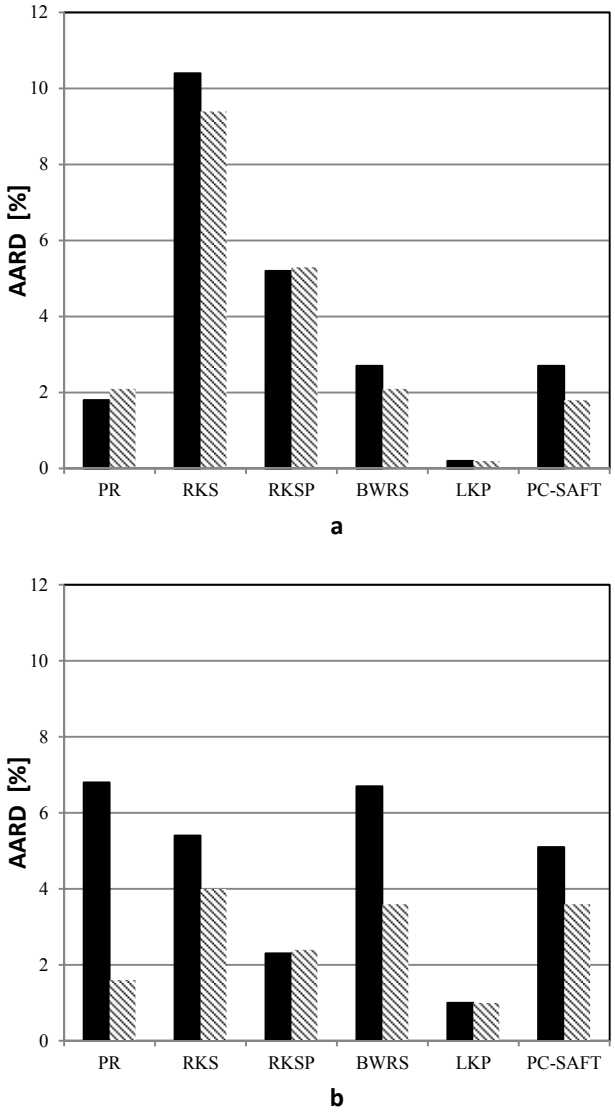

Fig. 3. AARDs between the liquid experimental density and the density calculated by EOS with k_{ij} defined in Aspen by default (■) and fitted k_{ij} (▨) for O_{2a} mixture (a) and for O_{2b} mixture (b).

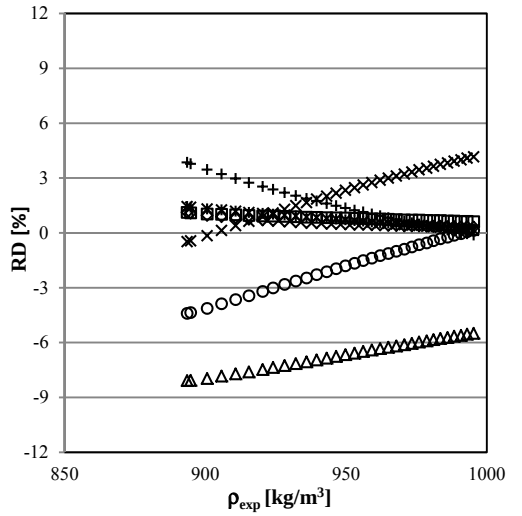

a

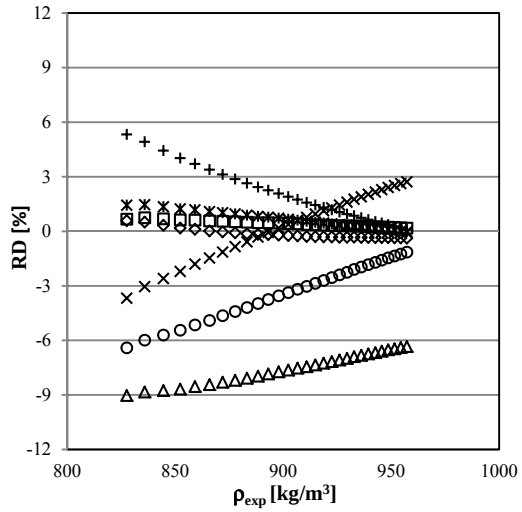

b

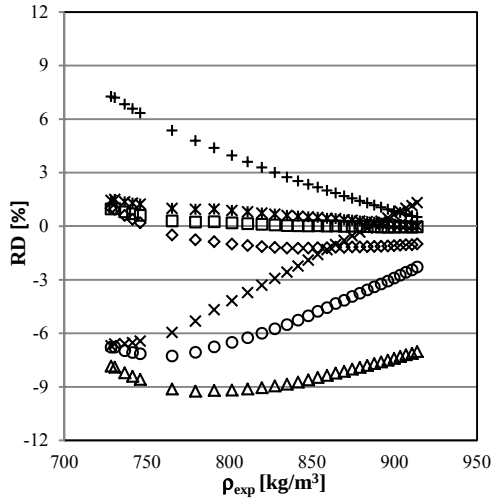

c

Fig. 4. RDs in terms of liquid density for selected EOS with fitted k_{ij} (except GERG model) against the experimental density value at 273.15 K (a), 283.15 K (b) and 293.15 K (c) for Ar_a mixture. x PR, Δ RKS, ○ RKSP, + BWRS, ∗ LKP, ◊ PC-SAFT, □ GERG.

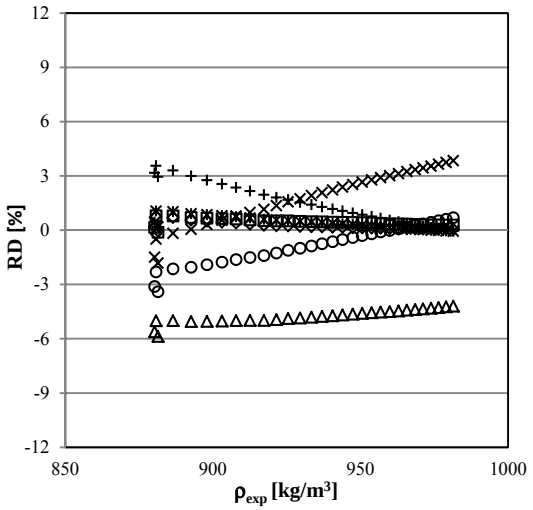

a

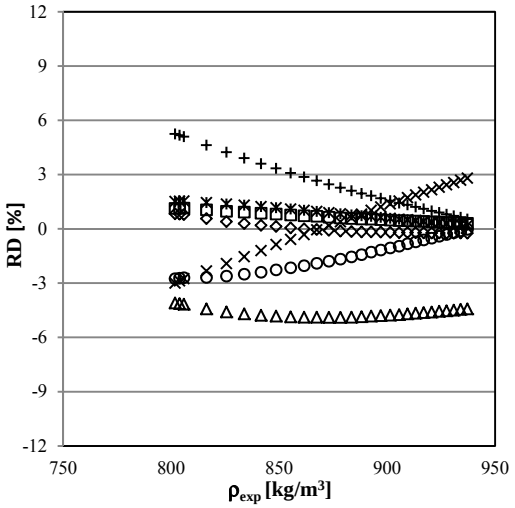

b

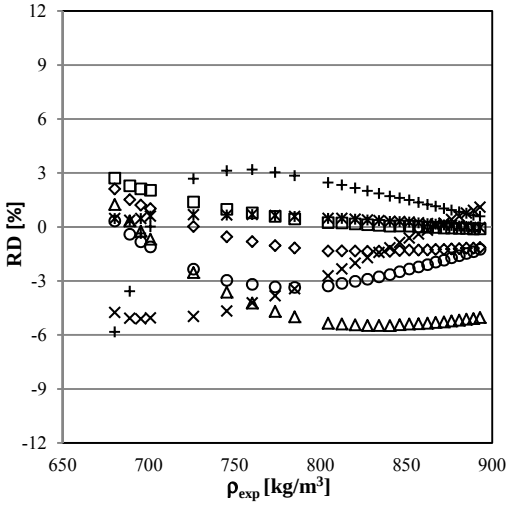

c

Fig. 5. RDs in terms of liquid density for selected EOS with fitted k_{ij} (except GERG model) against the experimental density value at 273.15 K (a), 283.15 K (b) and 293.15 K (c) for Ar_b mixture. x PR, Δ RKS, ○ RKSP, + BWRS, ∗ LKP, ◊ PC-SAFT, □ GERG.

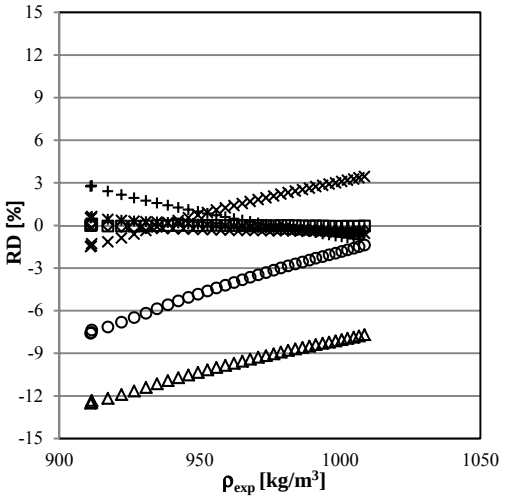

a

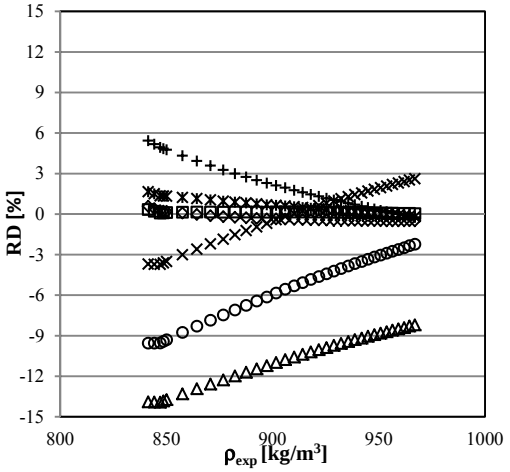

b

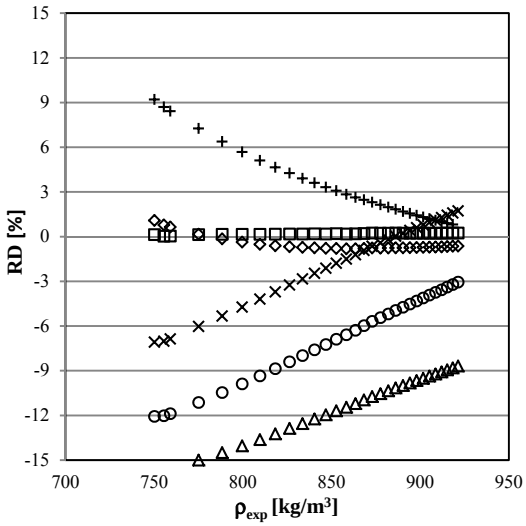

c

Fig. 6. RDs in terms of liquid density for selected EOS with fitted k_{ij} (except GERG model) against the experimental density value at 273.15 K (a), 283.15 K (b) and 293.15 K (c) for N_{2a} mixture. x PR, Δ RKS, ○ RKSP, + BWRS, ∗ LKP, ◊ PC-SAFT, □ GERG.

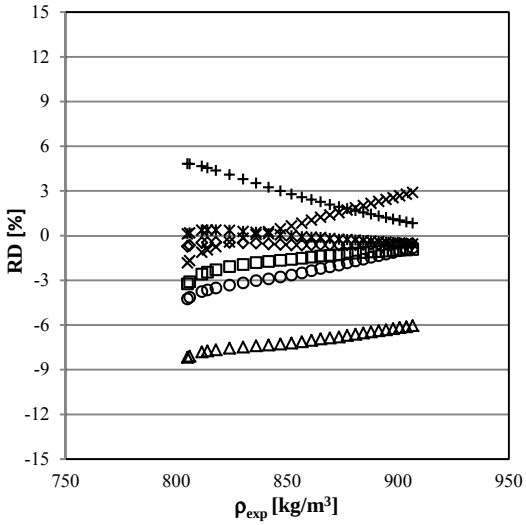

a

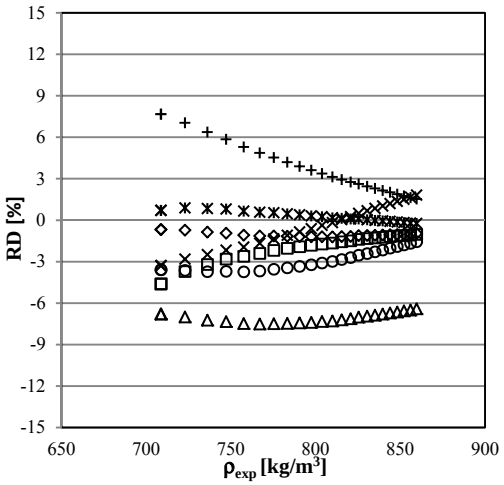

b

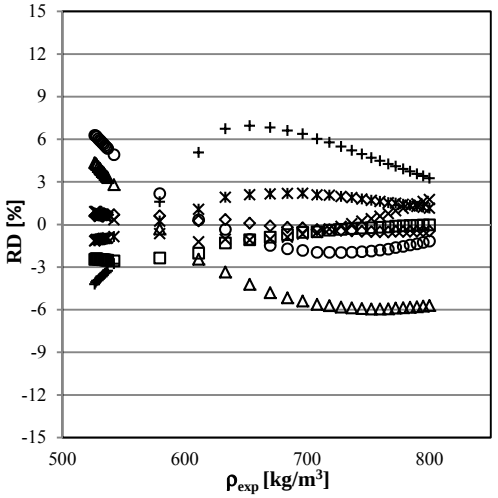

c

Fig. 7. RDs in terms of liquid density for selected EOS with fitted k_{ij} (except GERG model) against the experimental density value at 273.15 K (a), 283.15 K (b) and 293.15 K (c) for N_{2b} mixture. x PR, Δ RKS, ○ RKSP, + BWRS, ∗ LKP, ◊ PC-SAFT, □ GERG.

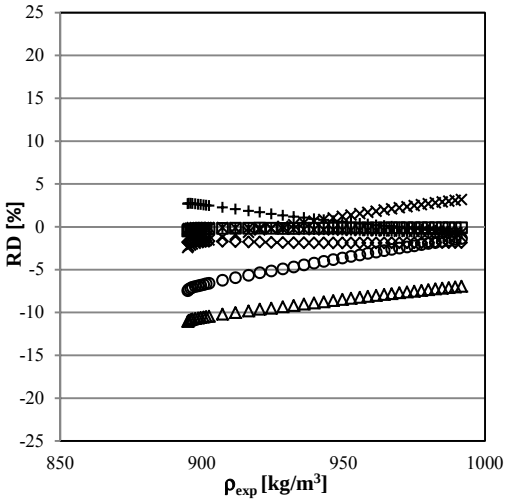

a

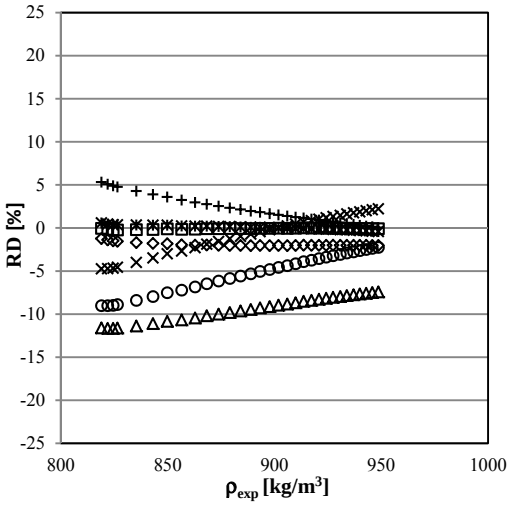

b

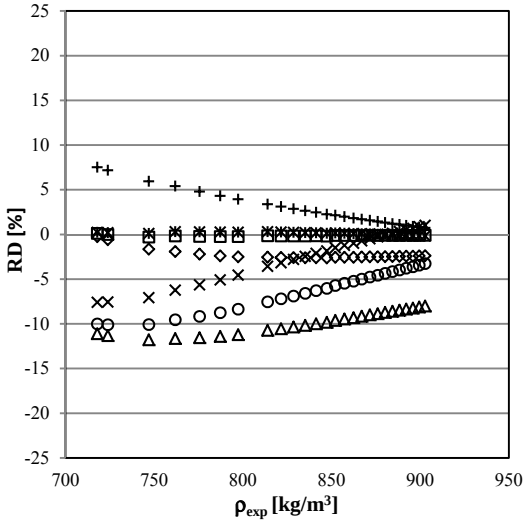

c

Fig. 8. RDs in terms of liquid density for selected EOS with fitted k_{ij} (except GERG model) against the experimental density value at 273.15 K (a), 283.15 K (b) and 293.15 K (c) for O_{2a} mixture. x PR, Δ RKS, ○ RKSP, + BWRS, ∗ LKP, ◊ PC-SAFT, □ GERG.

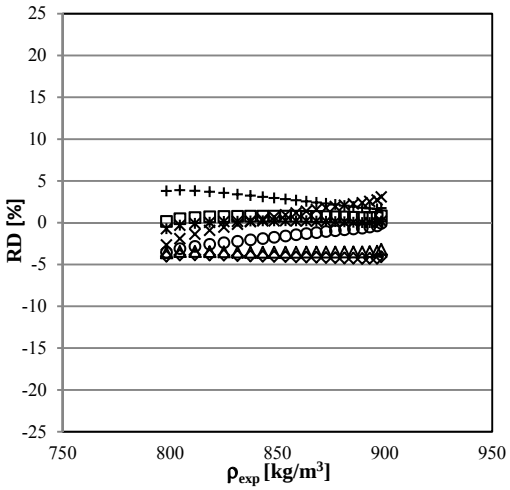

a

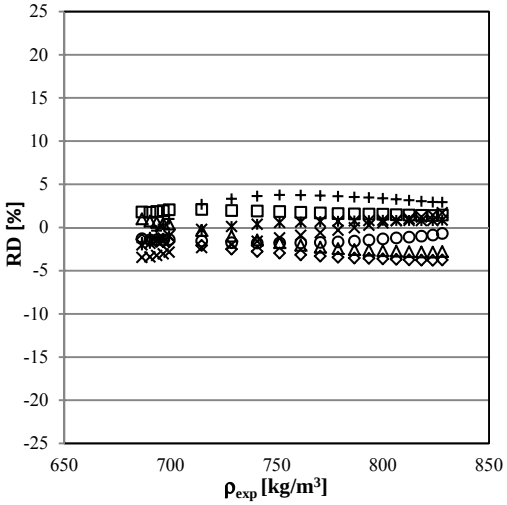

b

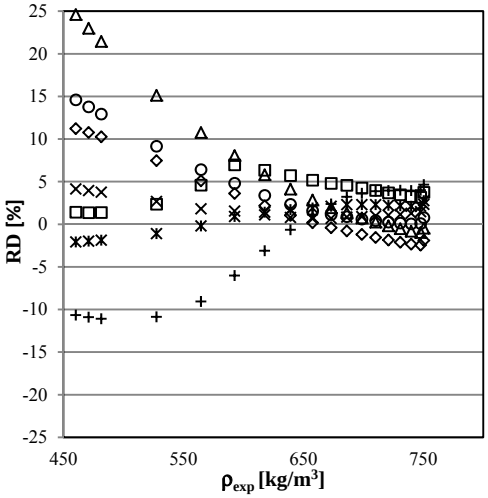

c

Fig. 9. RDs in terms of liquid density for selected EOS with fitted k_{ij} (except GERG model) against the experimental density value at 273.15 K (a), 283.15 K (b) and 293.15 K (c) for O_{2b} mixture. x PR, Δ RKS, ○ RKSP, + BWRS, ∗ LKP, ◊ PC-SAFT, □ GERG.

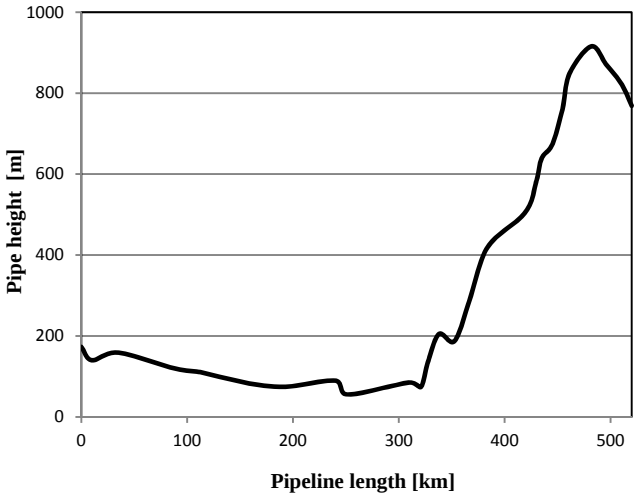

Fig. 10. Altimetric profile of simulated pipeline.

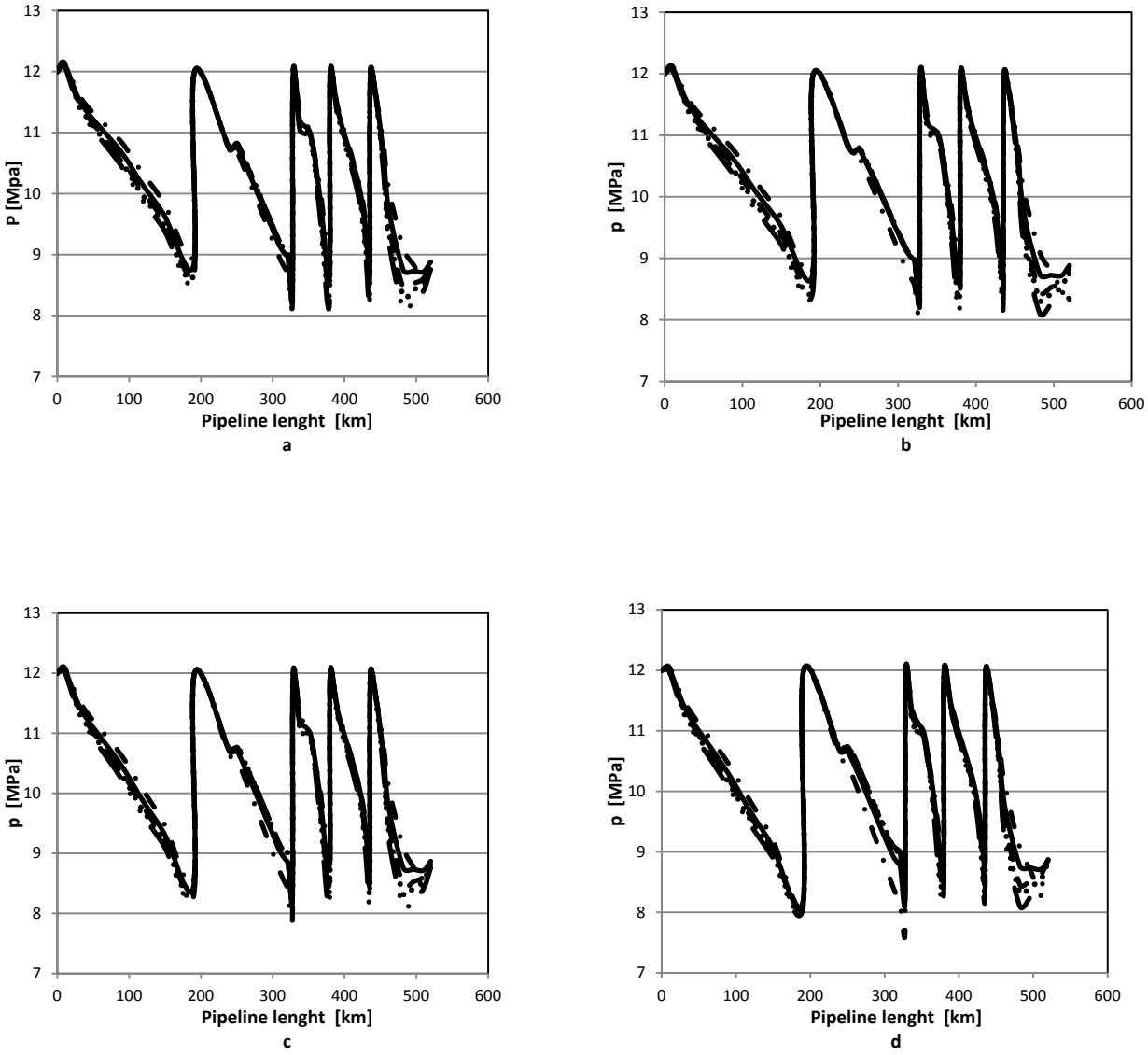

Fig. 11. The calculated pressure profile along the pipeline with $D = 0.618$ m for pure CO_2 at different ambient temperature, T_a. — . . — $T_a = 253$ K, ... $T_a = 273$ K, – – – – $T_a = 283$ K, ——— $T_a = 303$ K, – . – . . $T_a = 323$ K. and at different inlet fluid temperature, T_i. $T_i = 273$ K (a), $T_i = 283$ K (b), $T_i = 293$ K (c), $T_i = 303$ K (d)

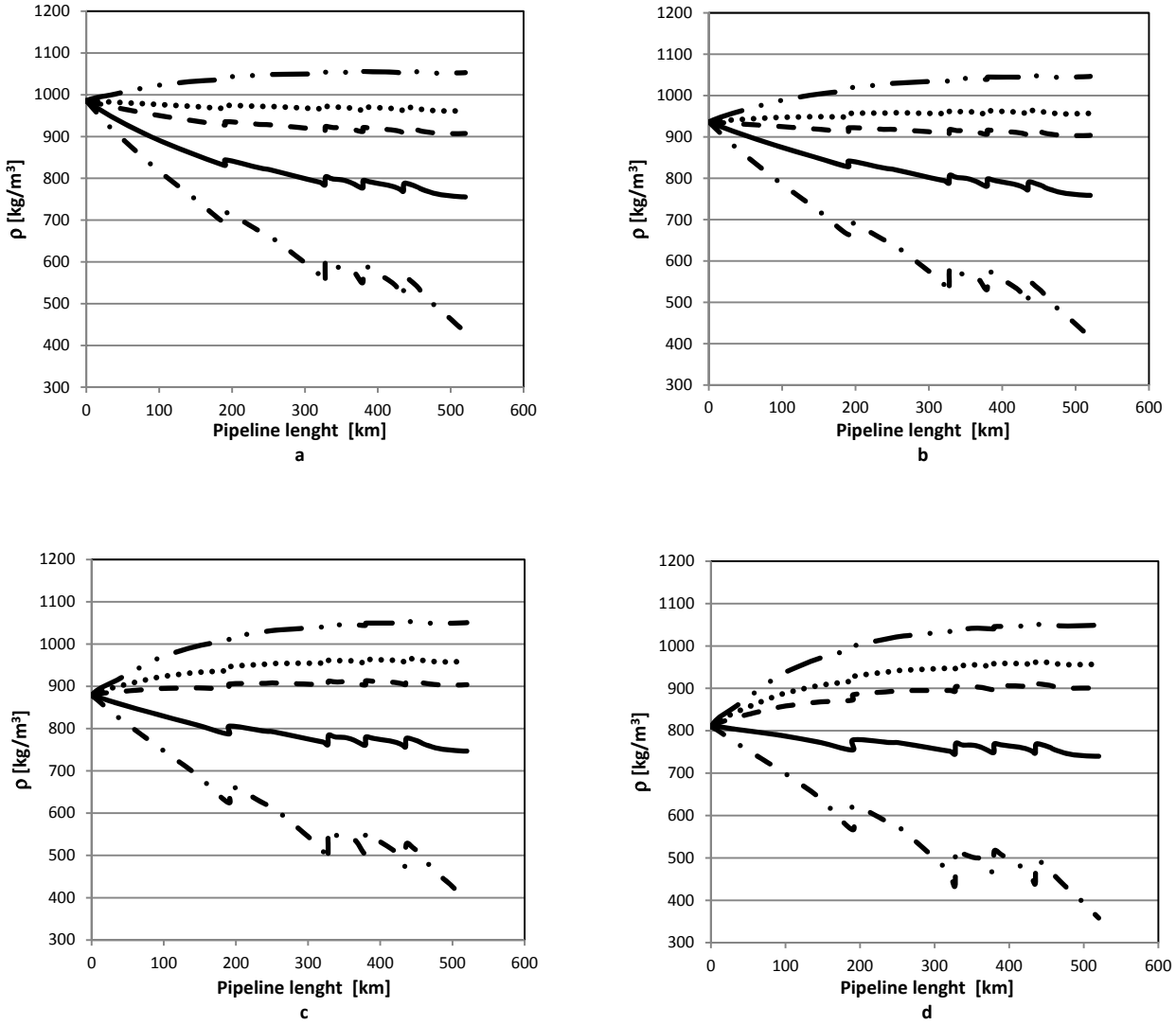

Fig. 12. The density profile along the pipeline with $D = 0.618$ m for pure CO_2 at different ambient temperature, T_a. — · · — $T_a = 253$ K, ... $T_a = 273$ K, - - - - $T_a = 283$ K, ——— $T_a = 303$ K, — · — · · $T_a = 323$ K. and at different inlet fluid temperature, T_i. $T_i = 273$ K (a), $T_i = 283$ K (b), $T_i = 293$ K (c), $T_i = 303$ K (d).

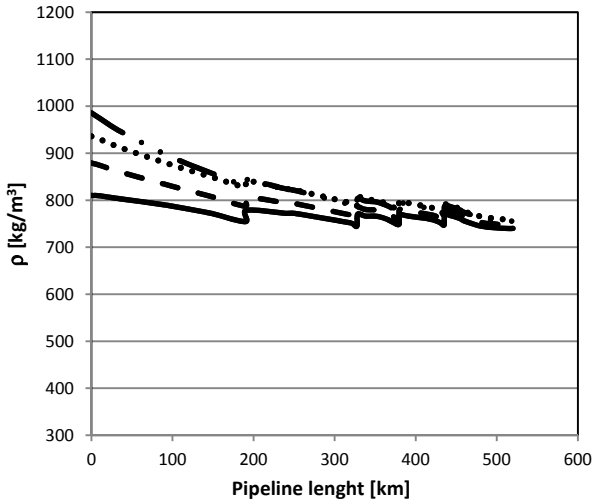

Fig. 13. The density profile along the pipeline with D = 0.618 m for pure CO_2 at T_a = 303 K and different inlet fluid temperature, T_i. — . . — T_1 = 273 K, ... T_i = 283 K, – – – – T_i = 293 K, ——— T_i = 303 K.

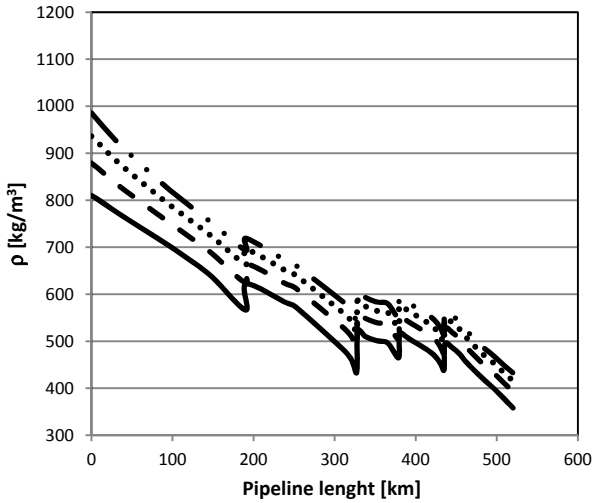

Fig. 14. The density profile along the pipeline with D = 0.618 m for pure CO_2 at T_a = 323 K and different inlet fluid temperature, T_i. — . . — T_1 = 273 K, ... T_i = 283 K, – – – – T_i = 293 K, ——— T_i = 303 K.

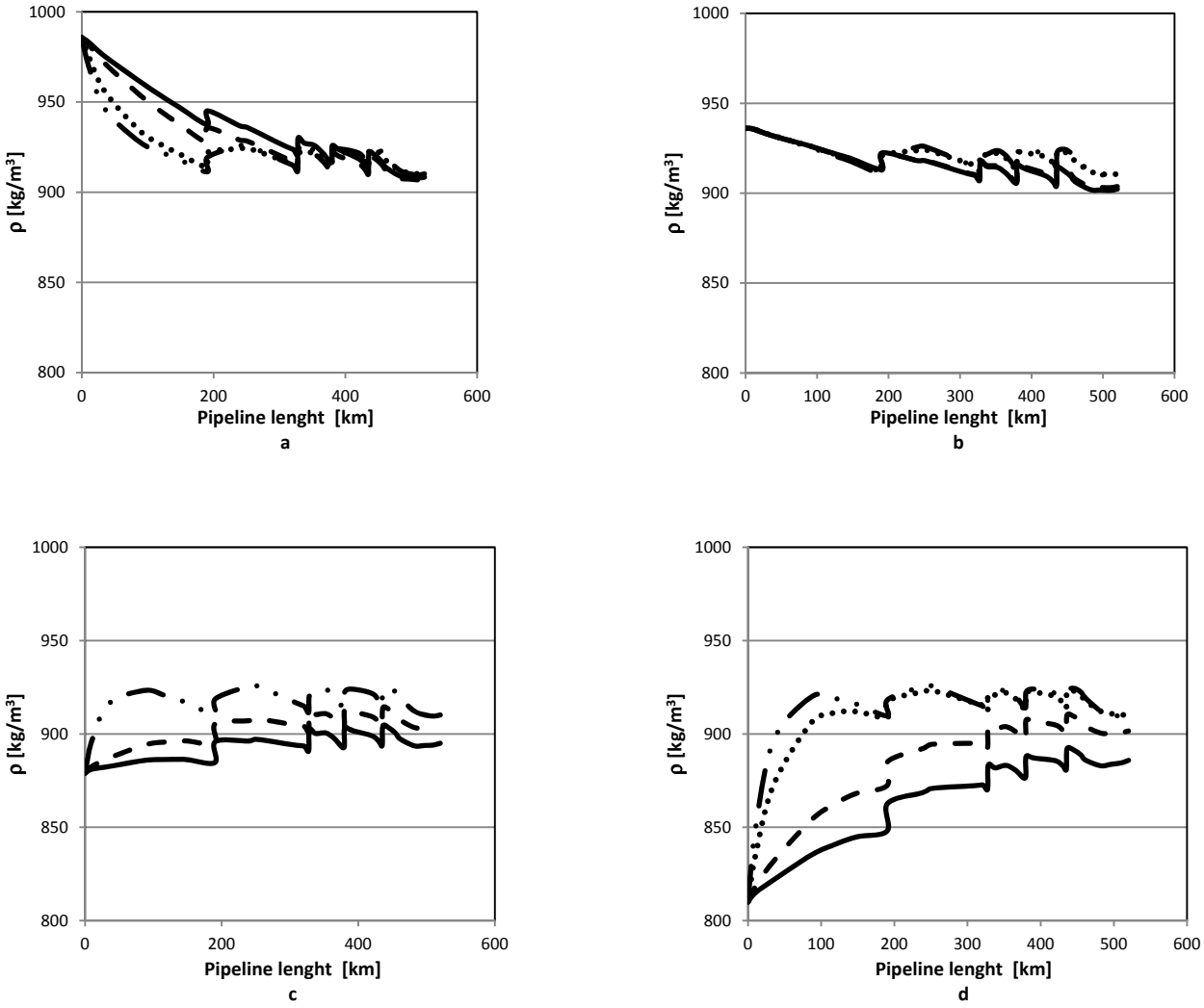

Fig. 15. The density profile along the pipeline for pure CO_2 with various diameters, D ⎯ . . ⎯ D= 0.303 m, ... D = 0.381 m, _ _ _ _D = 0.618 m, ——— D = 0.762 m at T_a.= 283 K and at different inlet fluid temperature, T_i. T_i = 273 K (a), T_i = 283 K (b), T_i = 293 K (c), T_i = 303 K (d).

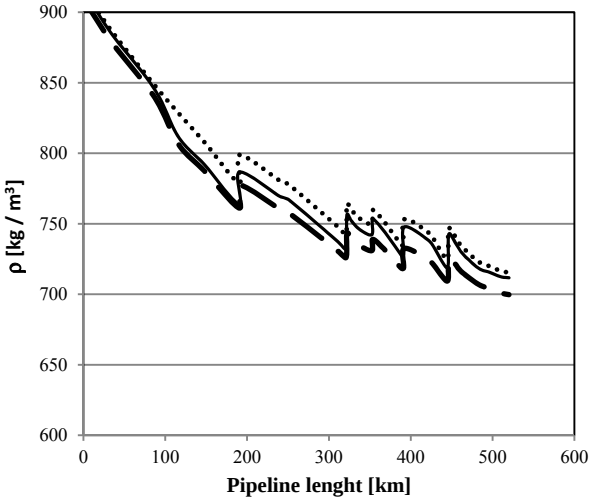

Fig. 16. The density profile along the pipeline for CO_2-Ar with x_{Ar} = 0.04 at T_a = 303 K for different EOS. ..... LKP equation, ___GERG model, _ _ PC-SAFT equation.

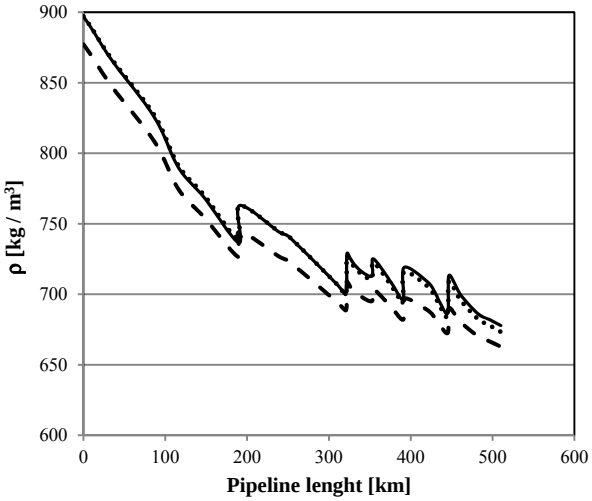

Fig. 17. The density profile along the pipeline for CO_2-O_2 with x_{O2} = 0.05 at T_a = 303 K for different EOS. ..... LKP equation, ___GERG model, _ _ PC-SAFT equation.

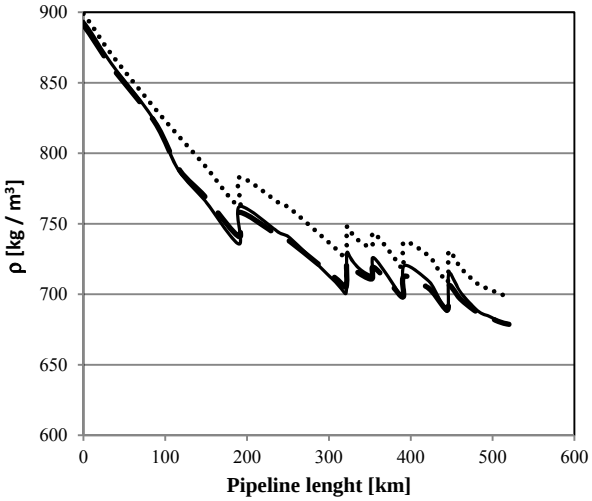

Fig. 18. The density profile along the pipeline for CO_2-N_2 with x_{N2} = 0.04 at T_a = 303 K for different EOS. ..... LKP equation, ___GERG model, _ _ PC-SAFT equation.

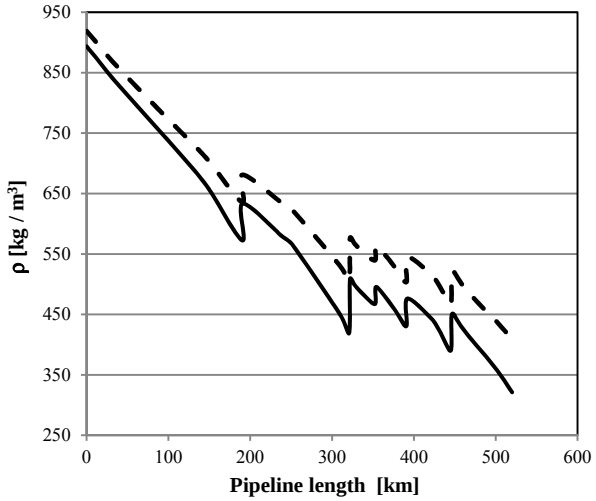

Fig. 19. The density profile along the pipeline for CO_2-N_2 mixture with different nitrogen molar fraction, x_{N2}, at T_a = 323 K obtained by simulation using GERG model. ——— x_{N2} = 0.02, – – –, x_{N2} = 0.04.

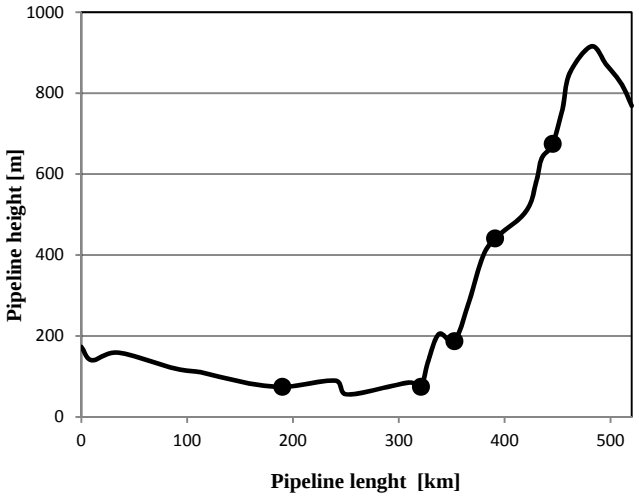

Fig. 20. Altimetric profile of pipeline configuration with five pumps (●).

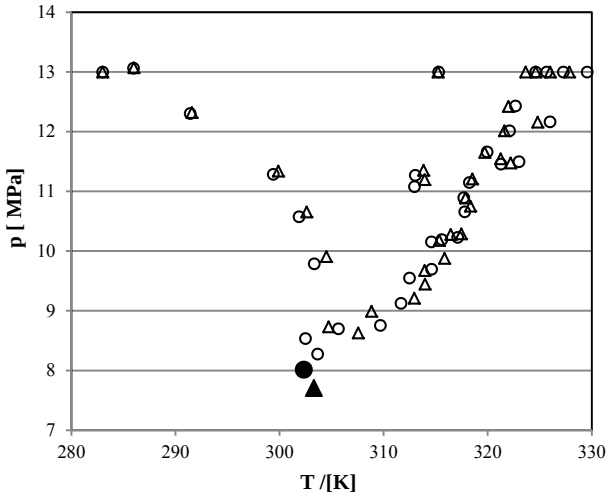

Fig. 21. The pressure and temperature values along the pipeline as regards the mixture critical point for CO_2-Ar mixture with different argon molar fraction, x_{Ar}, at T_a = 323 K. Δ x_{Ar} = 0.02, ○ x_{Ar} = 0.04, ▲critical point of CO_2-Ar mixture with x_{Ar} = 0.02, ● critical point of CO_2-Ar mixture with x_{Ar} = 0.04.